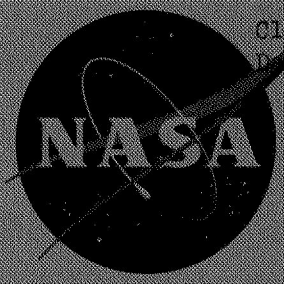

TECHNICAL MEMORANDUM

PERFORMANCE OF THREE ISENTROPIC ALL-INTERNAL-COMPRESSION AXISYMMETRIC INLETS DESIGNED FOR MACH 2.5

By Bernhard H. Anderson and David N. Bowditch

Lewis Research Center
Cleveland, Ohio

NATIONAL AERONAUTICS AND SPACE ADMINISTRATION
WASHINGTON September 1960

NATIONAL AERONAUTICS AND SPACE ADMINISTRATION

TECHNICAL MEMORANDUM X-259

PERFORMANCE OF THREE ISENTROPIC ALL-INTERNAL-COMPRESSION AXISYMMETRIC INLETS DESIGNED FOR MACH 2.5*

By Bernhard H. Anderson and David N. Bowditch

SUMMARY

An experimental investigation of three all-internal-compression inlets designed for Mach 2.5 and differing only in the length of the supersonic diffuser was conducted at Mach numbers 2.5 and 2.0 at angles of attack from 0° to 12°. The study was conducted to determine an optimum bleed system, to study starting at supersonic speeds, and to investigate inlet control parameters for all-internal-compression inlets.

The best bleed system for each of the three inlets incorporated a ram scoop on the cowl and a flush bleed on the centerbody located opposite each other immediately downstream of the throat. At Mach 2.5, a maximum pressure recovery of 0.926 was obtained with the intermediate-length inlet incorporating the cowl ram scoop. During starting, large amounts of cowl bleed were found necessary to cancel strong compressions from the centerbody. These strong compressions caused separation and prevented the attainment of design internal supersonic compression at Mach 2.5. Increased inlet tolerance to changes in Mach number and angle of attack was obtained by increasing porous bleed just upstream of the throat. The terminal shock affected the static pressure upstream of the throat, thereby making it difficult to use throat static pressure as a control signal to position the centerbody. However, the throat static pressure appears to be a useful signal for regulating the inlet corrected weight flow at Mach 2.5.

INTRODUCTION

One approach to reduce high cowl wave drag associated with high Mach number inlets is to make use of all-internal compression. Results from previous investigations indicate that high pressure recoveries and low cowl drag can be obtained with internal-compression inlets (refs. 1 to 5). Unfortunately, the internal-compression inlet has some design problems, such as starting and boundary-layer control.

*Title, Unclassified.

Results from a previous investigation (ref. 6) indicated that good performance could be obtained with a relatively long isentropic inlet at Mach 2.5. It was reported in reference 6 that an inlet half as long gave poor performance because it unstarted as the centerbody was retracted toward the design position at Mach 2.5. Apparently the coalescence of the isentropic compressions caused separation on the centerbody and prevented its retraction.

Since it was felt that the shorter inlet could be started by using large amounts of cowl bleed, three all-internal-compression inlets, differing only in the supersonic-diffuser length, were tested. The long and the short inlets were geometrically the same inlets as in reference 6 but with different bleed systems. The investigation was conducted in the 10- by 10-foot supersonic wind tunnel at the NASA Lewis Research Center. The three axisymmetric inlets had isentropic compression surfaces on the centerbody and cowl, designed for Mach 2.5. Available in combination for each of the three inlets were flush bleed, ram bleed, and porous bleed. Comparisons of inlet performance for each of the three inlets were made at Mach 2.5 and 2.0, with angles of attack ranging from 0° to 12°. Other data for the same three inlets are reported in reference 7.

SYMBOLS

A	flow area, sq ft
A_c	capture area, sq ft
M	Mach number
m	mass flow, slugs/sec
m_{cb}	cowl-bleed mass flow, slugs/sec
m_{cbb}	centerbody-bleed mass flow, slugs/sec
m_0	capture mass flow, $\rho_0 V_0 A_c$, slugs/sec
P	total pressure, lb/sq ft
$\overline{P}$	average total pressure, lb/sq ft
ΔP_2	maximum minus minimum total pressure at station 2
p	static pressure, lb/sq ft

Δp	maximum minus minimum static pressure during buzz
V	velocity, ft/sec
w	weight flow, lb/sec
$w\sqrt{\theta}/\delta A$	corrected weight flow, (lb/sec)/sq ft
α	angle of attack, deg
δ	ratio of total pressure to NASA standard sea-level pressure of 2116 lb/sq ft
θ	ratio of total temperature to NASA standard sea-level temperature of 518.7° R
ρ	density, lb/cu ft or slugs/cu ft

Subscripts:

0	free-stream conditions
1	throat station
2	diffuser-exit station
3	model-exit station

APPARATUS AND PROCEDURE

A cutaway view of the intermediate supersonic inlet showing the translating centerbody and the optimum bleed configuration is presented in figure 1. The model was designed so that the three inlets could be used interchangeably with the rear section. The throat section of the model (station 1) could be assembled so that either a flush bleed slot or a ram scoop could be used in combination with each of the three inlets. Three plugs located in the rear of the model metered the main diffuser mass flow, while the two upper plugs metered the cowl- and centerbody-bleed flows.

Detailed schematic diagrams of the three inlets are shown in figure 2, and their coordinates are shown in tables I and II. The dimensions of the long inlet are shown in figure 2(a). The manner in which the theoretical contours of the isentropic compression surfaces were determined is described in reference 6. Three cowl-bleed configurations were tested with the long inlet, two flush slots of different dimensions

and a ram scoop. A flush bleed slot was located on the centerbody in the same plane as the cowl bleed when the centerbody was in the design position for Mach 2.5. One and four rows of porous bleed located just ahead of the throat were tested. The porous bleed consisted of 1/8-inch-diameter holes drilled perpendicular to the centerline of the inlet. The holes were staggered, with 0.188 inch between hole centerlines in each row.

The intermediate inlet (fig. 2(b)) had a supersonic-diffuser length 7/10 of that of the long inlet. Both a cowl flush slot and a cowl ram scoop were tested with the intermediate inlet. The dimensions of the cowl bleeds are shown in figure 2(b). A flush slot was located on the centerbody opposite the cowl bleed when the centerbody was located in the Mach 2.5 design position. Available with the cowl flush and ram-scoop bleed was porous bleed upstream of the throat. The porosity of the bleed could be varied by means of a rotating sleeve that fitted over the outside of the cowl. The sleeve was match-drilled with the cowl; therefore, by rotating the cowl sleeve, the bleed-flow area could be changed. Upstream of the perforated bleed section, two rows of holes were drilled in the cowl inclined to the inlet centerline at 20° and 30°, respectively.

The short inlet, which is shown in figure 2(c), had a supersonic-diffuser length half as long as the long inlet and a maximum design pressure gradient three times that of the long inlet. A ram scoop and a 0.130-inch flush slot were tested on the cowl of the short inlet. The porous bleed forward of the throat could be varied by means of a rotating sleeve similar to the one used with the intermediate inlet. One row of holes located ahead of the rotating sleeve and inclined 20° to inlet centerline was used for additional supersonic bleed. A flush bleed slot located on the centerbody was used with all cowl-bleed configurations. The baffles on the outside of the inlets surrounding the porous and starting bleed holes were used to ensure a low pressure on the discharge side.

Coordinates for the isentropic cowls and centerbodies are presented in tables I and II. Two centerbodies were used with the long inlet. The long inlet, using spike B, had a 3.46-percent-larger throat area than the long inlet using spike A, which in turn had a 2.67-percent-larger throat area than the long inlet described in reference 6. The internal-flow area for various centerbody positions is presented in figure 3 for the configurations of primary importance.

The inlet pressure recovery and distortion were measured at the diffuser exit (station 2) by 36 area-weighted total-pressure tubes in six rakes and three wall static-pressure orifices. Distortions were determined from the difference between the maximum and minimum total pressures divided by the average total pressure. Flow conditions in

the throat were measured with a rake of eight total-pressure tubes and three static-pressure orifices. The rake was removed before recording diffuser-exit data. A translating Pitot static-pressure probe (located in the throat) was connected to a pressure transducer and was moved through the throat to obtain the longitudinal variation in static pressure near the terminal shock.

The inlet mass-flow and bleed-flow ratios were computed from the measured static pressures at station 3 and the known sonic discharge areas, assuming isentropic flow between station 3 and the respective choked discharge areas. Supersonic bleed mass flow was assumed to be the difference between the known capture mass flow and the sum of the measured mass flows.

The Mach number and angle-of-attack tolerance ΔM and $\Delta\alpha$ were obtained by lowering the test-section Mach number or increasing the angle of attack until the inlet unstarted. This was done with the centerbody in the design position for Mach 2.5.

RESULTS AND DISCUSSION

General Inlet Performance

A summary of the inlet configurations, showing inlet performance for peak pressure recovery at Mach 2.5, is presented in table III. A maximum pressure recovery of 0.926 was obtained with the intermediate inlet using a cowl ram scoop. The cowl ram scoop generally provided the maximum pressure recoveries with each inlet configuration but at the expense of relatively high bleed mass-flow ratios. Table IV presents the peak-pressure-recovery performance for the long inlet at Mach 2.0. For each of the configurations listed, the centerbody was located forward of the Mach 2.5 design position. Total-pressure contours for peak pressure recovery at the diffuser exit (station 2) are presented in figure 4 for the long, intermediate, and short inlets with cowl ram bleed. The distortions between the three inlets were about equal and were generally radial in nature at peak inlet recovery. These distortions are typical for other types of bleed at peak inlet recovery.

Bleed Performance

The effect of ram-scoop bleed on inlet performance for Mach 2.5 and 2.0 is presented in figure 5. The inlet total-pressure recovery as a function of cowl- and centerbody-bleed flow was obtained with maximum centerbody- and cowl-bleed flow, respectively. At Mach 2.5, the cowl ram-scoop bleed flow could not be turned off because the terminal shock

would be expelled. For the long and intermediate inlets, the total-pressure recovery increased at a rapid rate with increasing cowl bleed. The intermediate inlet recovery reached 0.92 at a cowl-bleed mass-flow ratio of 0.06, and further bleed produced small changes in recovery. The recovery for the long inlet, however, rose continuously with cowl bleed to a maximum pressure recovery of 0.904 at a bleed mass-flow ratio of 0.076. The centerbody bleed did not affect the total-pressure recovery as much for the long inlet as for the intermediate inlet, which has a higher rate of compression.

Maximum mass-flow ratio m_1/m_0 at which the inlets could be operated was 0.99 for the long inlet and 0.95 and 0.93 for the intermediate and short inlets, respectively. The short inlet generally gave the poorest performance of the three inlets. At Mach 2.0 the insensitivity of the ram bleed for the intermediate inlet (open square symbols) was caused by the ram scoop's being well downstream of the terminal shock. By opening the sleeve bleed on the intermediate inlet (solid square symbols), it was possible to retract the centerbody into Mach 2.5 design position at Mach 2.0. However, the mass-flow ratio was thereby reduced from 0.75 to 0.65, a value considerably lower than that for the long inlet (0.84).

The effect of flush bleed on the inlet performance is presented in figure 6 for Mach 2.5 and 2.0. Inlet total-pressure recoveries are presented as functions of centerbody- and cowl-bleed mass flow at maximum cowl- and centerbody-bleed flows, respectively. With the long inlet and small flush slot (0.114 in.), the total-pressure recovery was increased from a value of 0.832 to 0.87 by increasing the cowl-bleed mass-flow ratio from zero to 0.05 at Mach 2.5. Increasing the centerbody-bleed mass-flow ratio beyond 0.01 with maximum cowl bleed tended to lower total-pressure recovery. With the long inlet and large flush slot (0.184 in.), 2.5 counts in total-pressure recovery were gained by increasing the cowl-bleed mass-flow ratio from the small-slot value of 0.05 to 0.09.

Cowl bleed on the short inlet did not appreciably change the total-pressure recovery at Mach 2.5, but increasing centerbody-bleed mass-flow ratio from zero to 0.03 increased the total pressure 3 counts. At Mach 2.0, a pressure recovery of 0.78 was obtained with the short inlet. Opening the cowl porous bleed allowed the centerbody to be retracted from 0.888 to 0.635 inlet diameter and raised the recovery to 0.88. However, the cowl bleed exceeded the additional mass flow captured, and the mass-flow ratio m_1/m_0 decreased about 1 percent.

Off-Design Performance

The effect of angle of attack on peak pressure recovery is presented in figure 7 for Mach 2.5 and 2.0. The manner in which the total-pressure recovery decreased with increasing angles of attack was similar for each of the configurations tested. At Mach 2.5, the angle of attack was increased with the centerbody in the Mach 2.5 design position (zero centerbody extension). The centerbody was kept at zero extension until an angle of attack was reached where the terminal shock could no longer remain swallowed. Remaining data were obtained at the maximum centerbody retraction with the inlet started.

A summary of maximum-angle-of-attack and Mach number tolerance is presented in table V. The Mach number tolerance is defined as the maximum decrease in Mach number from 2.5 that could be attained, with the centerbody remaining at zero extension, without expelling the terminal shock. Increasing the amount of porous bleed forward of the throat from one to four rows increased the maximum angle of attack from 3.55° to 6.75° and the Mach number tolerance from ΔM of 0.07 to 0.10, without any appreciable change in total-pressure recovery. By increasing the throat area 3.46 percent by using centerbody B, the maximum angle of attack was increased from 3.40° to 5.25°, and Mach number tolerance was increased from 0.06 to 0.10. The 3.46-percent change in area ratio, however, resulted in a 2.5-count loss in total-pressure recovery at peak conditions.

Starting

At Mach 2.5, the intermediate and short inlets unstarted as the centerbody was retracted into the design position with the porous bleed controlled by the sleeve (at max. porosity). The misalinement between the compression surfaces during starting was believed to have caused the isentropic compressions to coalesce into strong shocks, which separated the flow on the centerbodies. Therefore, additional cowl-bleed holes were incorporated forward of the porous-bleed section to cancel the disturbing shocks. The two rows of additional bleed holes located upstream of the sleeve bleed on the intermediate inlet and one row on the short inlet allowed the centerbodies to be retracted into the Mach 2.5 design position. Once the centerbody was in the design position, the additional bleed flow amounted to about 1.5 percent of the total mass flow.

The starting cycle for the long inlet at zero angle of attack is presented in figure 8. Corrected weight flow, average total-pressure recovery, and buzz amplitude ratio are presented as a function of centerbody position. The inlet was unstarted by a small decrease in the plug discharge area with the centerbody fully retracted (going from point A

to point B). The average total-pressure recovery decreased from 0.870 (point A) to 0.480 (point B). The corrected weight flow was then increased (by increasing the plug discharge area) to 32.6 pounds per second per square foot, which was the minimum required for starting (point C). The centerbody was then extended until the inlet started (point D). After starting the inlet, the centerbody was retracted to the design position, with the exit plugs positioned to give the peak pressure recovery at each centerbody position (circular symbols).

With the inlet started there were no shock instabilities. However, some buzz was obtained with the inlet unstarted, and these data are presented in the lower part of the figure for two values of corrected weight flow, 32.6 (min. required for starting) and 29.6 (value at peak pressure recovery with centerbody in design position). A maximum buzz amplitude of 35 percent of the free-stream static was measured for the restart cycle.

Inlet Control

The static pressure measured in the throat of the long inlet with a translating probe is presented in figure 9 for three inlet total-pressure recoveries and centerbody B in the design Mach 2.5 position. At peak pressure recovery (0.878), the shock train appears to have consolidated over the bleed slots, which are in line with each other (fig. 9(a)). As the shock train moved downstream (decreasing total-pressure recovery), the static pressure forward of the bleed slots decreased (figs. 9(b) and (c)). Because the static pressure ahead of the throat is affected by the shock position, it would be difficult to use a throat pressure-ratio control to position the centerbody for peak performance. However, the throat static pressure is a potentially useful signal for a control that regulates inlet corrected weight flow.

CONCLUDING REMARKS

From an investigation of three all-internal-compression axisymmetric inlets differing only in the length of the supersonic diffuser, the following results were obtained:

1. At Mach 2.5 a maximum pressure recovery of 0.926 was obtained with the intermediate inlet incorporating a ram bleed on the cowl and flush bleed on the spike.

2. Ram-scoop bleed on the cowl generally gave the highest pressure recovery with each of the three inlets tested, but at a relatively high bleed mass-flow ratio.

3. Increasing porous bleed from one to four rows on the cowl in the supersonic diffuser increased the tolerance of the inlet to changes in free-stream Mach number and angle of attack.

4. The terminal shock affected the static pressure upstream of the throat, thereby making it difficult to use a throat pressure-ratio control to position the centerbody; however, the throat stream static pressure appears to be a useful signal for controlling the inlet corrected weight flow at Mach 2.5 and 0° angle of attack.

Lewis Research Center
National Aeronautics and Space Administration
Cleveland, Ohio, April 11, 1960

REFERENCES

1. Mossman, Emmet A., and Pfyl, Frank A.: An Experimental Investigation at Mach Numbers from 2.1 to 3.0 of Circular-Internal-Contraction Inlets with Translating Centerbodies. NACA RM A56G06, 1956.

2. Kepler, C. E.: Performance of a Variable-Geometry Chin Inlet at Mach Numbers from 1.6 to 3.0. Rep. R-0955-24, United Aircraft Corp., Oct. 1957.

3. Hubbartt, J. E.: Preliminary Investigation of Isentropic Integral Contraction Inlets. Rep. LB 12229, Lockheed Aircraft Corp., Sept. 20, 1953.

4. Watson, Earl C.: An Experimental Investigation at Mach Numbers from 2.1 to 3.0 of Circular Internal-Compression Inlets Having Translatable Centerbodies and Provisions for Boundary-Layer Removal. NASA TM X-156, 1960.

5. Doering, D. A.: Experimental Investigation of Some Design Parameters for Axisymmetric Internal Compression and External-Internal-Compression Inlets at Mach 4.91. Rep. ZR 659-025, Convair (San Diego), July 28, 1959.

6. Bowditch, David N., and Anderson, Bernhard H.: Performance of an Isentropic, All-Internal-Contraction, Axisymmetric Inlet Designed for Mach 2.50. NACA RM E58E16, 1958.

7. Hubbartt, J. E.: Experimental Investigation of Three Mach 2.5 Isentropic, All-Internal-Contraction, Axisymmetric Inlets of Different Lengths. Rep. ER-3552, Lockheed Aircraft Corp., Dec. 31, 1958.

TABLE I. - COWL COORDINATES

Long cowl		Intermediate cowl		Short cowl	
Distance ahead of throat, in.	Cowl radius, in.	Distance ahead of throat, in.	Cowl radius, in.	Distance ahead of throat, in.	Cowl radius, in.
14.55	4.466	10.18	4.524	7.60	4.517
14.00	4.466	9.50	4.528	6.75	4.522
13.00	4.463	8.50	4.520	5.75	4.501
12.00	4.459	7.50	4.492	4.75	4.448
11.00	4.444	6.50	4.445	3.75	4.349
10.00	4.413	5.50	4.363	2.75	4.208
9.00	4.370	4.50	4.253	1.75	4.053
8.00	4.319	3.50	4.141	.75	3.968
7.00	4.262	2.50	4.024	0	3.949
6.00	4.201	1.50	3.973		
5.00	4.139	.50	3.949	Cylindrical rear of throat	
4.00	4.079	0	3.949		
3.00	4.023				
2.00	3.979	Cylindrical rear of throat			
1.00	3.954				
0	3.949				
Cylindrical rear of throat					

TABLE II. - CENTERBODY COORDINATES

[Centerbody B has 3.69%-larger throat area than spike A.]

(a) Forward of throat.

Long centerbody			Intermediate centerbody		Short centerbody	
Distance from throat, in.	Radius A, in.	Radius B, in.	Distance from throat, in.	Radius, in.	Distance from throat, in.	Radius, in.
-18.37	0	0	-14.77	0	-12.14	0
-18.00	.033	.030	-14.00	.039	-11.25	.073
-17.00	.108	.101	-13.00	.129	-10.25	.193
-16.00	.209	.198	-12.00	.252	-9.25	.349
-15.00	.337	.322	-11.00	.397	-8.25	.532
-14.00	.476	.458	-10.00	.561	-7.25	.748
-13.00	.623	.601	-9.00	.748	-6.25	.986
-12.00	.778	.752	-8.00	.953	-5.25	1.124
-11.00	.941	.911	-7.00	1.175	-4.25	1.509
-10.00	1.109	1.075	-6.00	1.409	-3.25	1.806
-9.00	1.288	1.250	-5.00	1.664	-2.25	2.125
-8.00	1.478	1.436	-4.00	1.947	-1.25	2.435
-7.00	1.681	1.635	-3.00	2.230	-.25	2.603
-6.00	1.890	1.840	-2.00	2.453	0	2.602
-5.00	2.086	2.032	-1.00	2.575		
-4.00	2.255	2.198	0	2.602		
-3.00	2.382	2.321				
-2.00	2.464	2.339				
-1.00	2.511	2.442				
0	2.532	2.459				

TABLE II. - Concluded. CENTERBODY COORDINATES

[Centerbody B has 3.69%-larger throat area than spike A.]

(b) Rearward of throat.

Long centerbody			Intermediate and short centerbodies	
Distance from throat, in.	Radius A, in.	Radius B, in.	Distance from throat, in.	Radius, in.
0	2.532	2.459	0	2.602
.804	2.532	2.459	.804	2.602
1.804	2.509	2.445	1.804	2.570
2.804	2.478	2.423	2.804	2.530
3.804	2.439	2.394	3.804	2.483
4.804	2.394	2.358	4.804	2.429
5.804	2.341	2.314	5.804	2.367
6.804	2.280	2.262	6.804	2.297
7.804	2.211	2.202	7.804	2.219
8.744	2.139	2.139	8.744	2.139
9.604	2.028	2.028	9.604	2.028
10.604	1.867	1.867	10.604	1.867
11.604	1.758	1.758	11.604	1.758
12.604	1.710	1.710	12.604	1.710
13.604	1.600	1.600	13.604	1.600

TABLE III. - INLET PERFORMANCE AT PEAK PRESSURE RECOVERY AT MACH 2.5

[Centerbody-throat bleed type, small flush slot.]

Inlet type	Cowl-throat bleed type	Peak pressure recovery, P_2/P_0	Total-pressure distortion, $\Delta P_2/\bar{P}_2$	Supersonic cowl-bleed mass-flow ratio	Cowl-throat bleed mass-flow ratio, m_{cb}/m_0	Centerbody-throat bleed mass-flow ratio, m_{cbb}/m_0	Mass-flow ratio, m_1/m_0
Long with centerbody A	Small flush slot	0.878	0.160	0.01	0.06	0.01	0.92
	Large flush slot	.896	.114	.012	.09	.03	.87
	Ram scoop	.904	.154	.01	.07	.04	.88
Intermediate	Ram scoop	0.926	0.148	0.04	0.08	0.03	0.85
Short	Ram scoop	0.888	0.156	0.05	0.12	0.02	0.81

TABLE IV. - LONG-INLET PERFORMANCE AT PEAK PRESSURE RECOVERY AT MACH 2.0

[Same centerbody flush slot for all configurations.]

Center-body	Cowl-throat bleed type	Porous-bleed rows	Centerbody position, inlet diam ahead of design	Peak pressure recovery, P_2/P_0	Total-pressure distortion, $\Delta P_2/\bar{P}_2$	Super-sonic cowl-bleed mass-flow ratio	Centerbody-throat bleed mass-flow ratio, m_{cbb}/m_0	Mass-flow ratio, m/m_0
A	Small flush slot	1	1.192	0.886	0.195	0.01	0.02	0.88
	Small flush slot	4	1.192	.877	.180	.01	.01	.83
	Ram scoop	1	1.204	.891	.211	.04	.01	.82
B	Large flush slot	1	1.236	0.886	0.177	0.01	0.01	0.86

TABLE V. - MACH NUMBER AND ANGLE-OF-ATTACK TOLERANCE FOR LONG INLET

Ratio of throat to cowl area	Cowl-throat bleed type	Cowl porous-bleed rows	Total-pressure recovery at $M_0 = 2.5$ and $\alpha = 0^\circ$, P_2/P_0	Mach number tolerance (ΔM from 2.5)	Max. angle of attack with 0 centerbody extension, α, deg
0.461	Large flush slot	1	0.895	0.06	3.40
	Small flush slot	1	.878	.07	3.55
	Small flush slot	4	.873	.10	6.75
0.478	Large flush slot	1	0.870	0.10	5.25

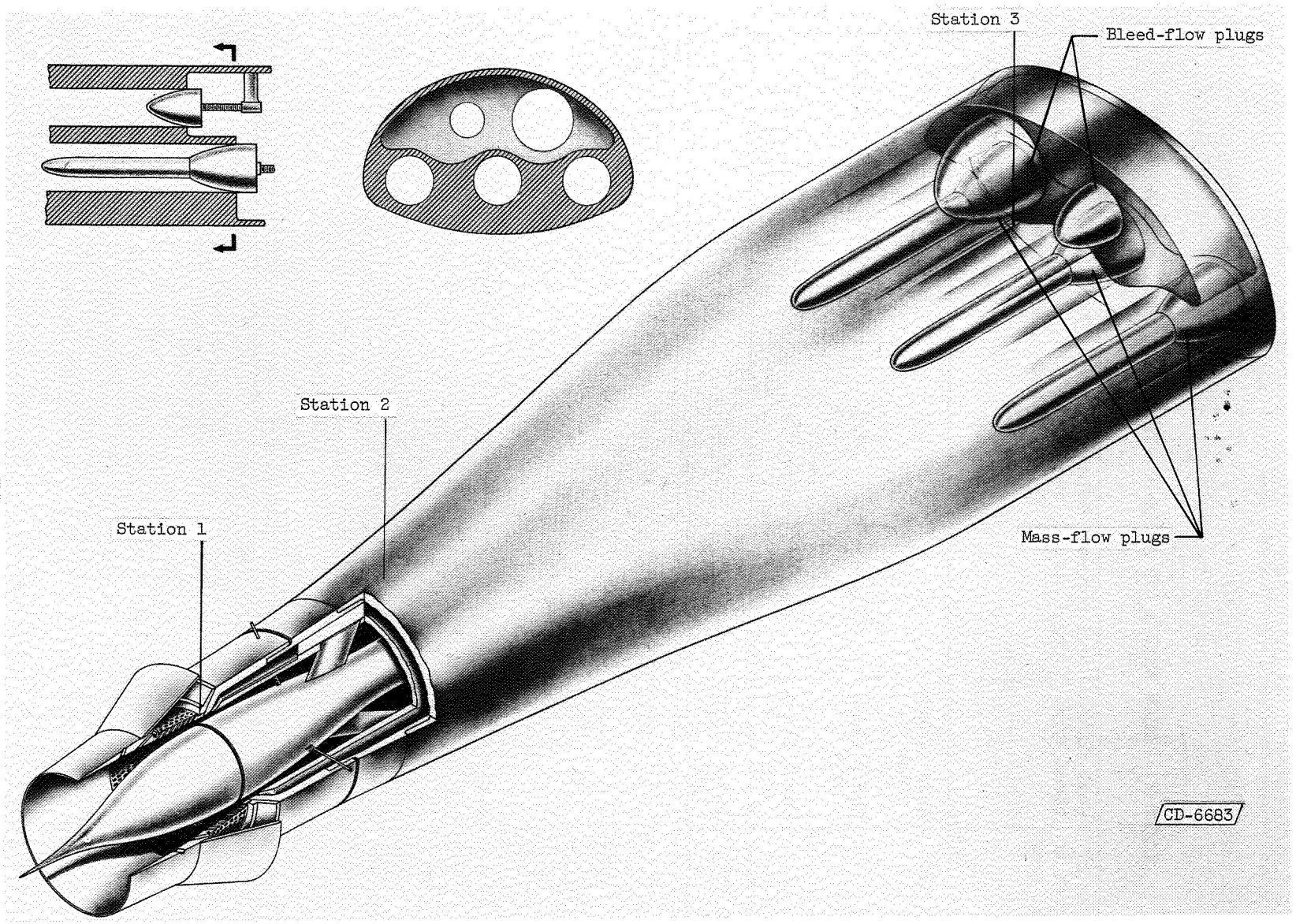

Figure 1. - Intermediate supersonic inlet with cowl ram scoop and porous bleed.

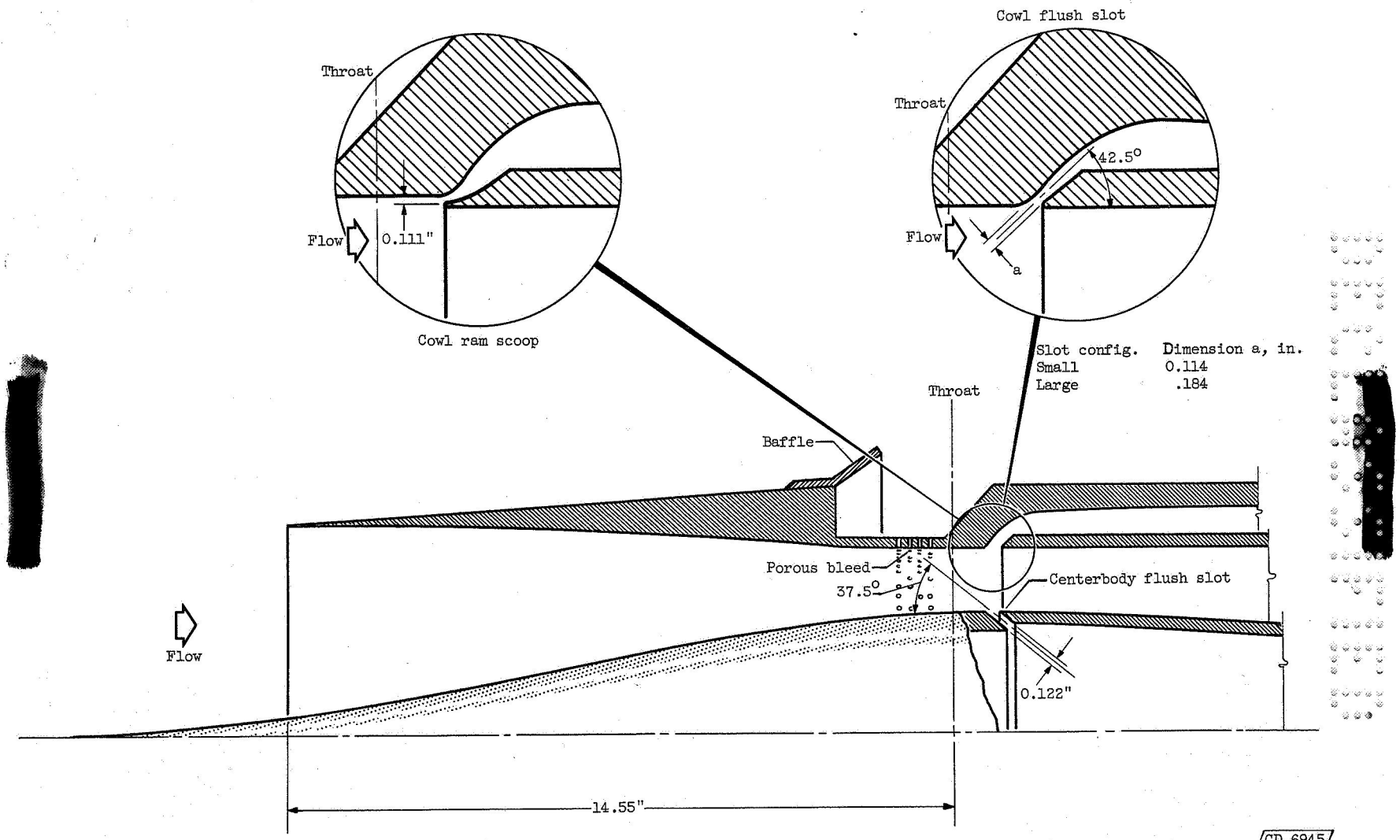

(a) Long supersonic inlet with bleed configurations (centerbody in design position).

Figure 2. - Schematic diagrams of inlets investigated.

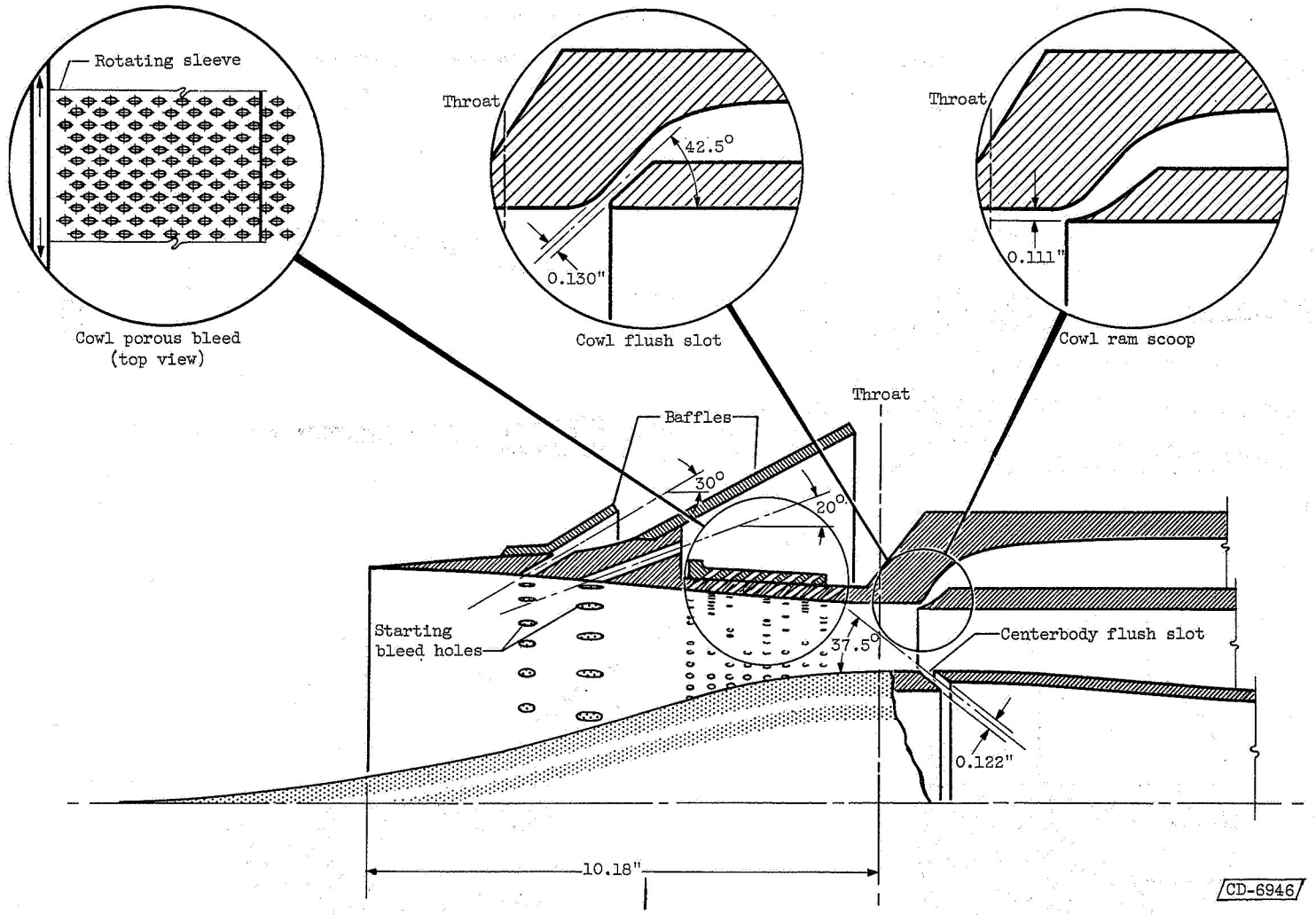

(b) Intermediate supersonic inlet with bleed configurations. (centerbody shown in design position).

Figure 2. - Continued. Schematic diagrams of inlets investigated.

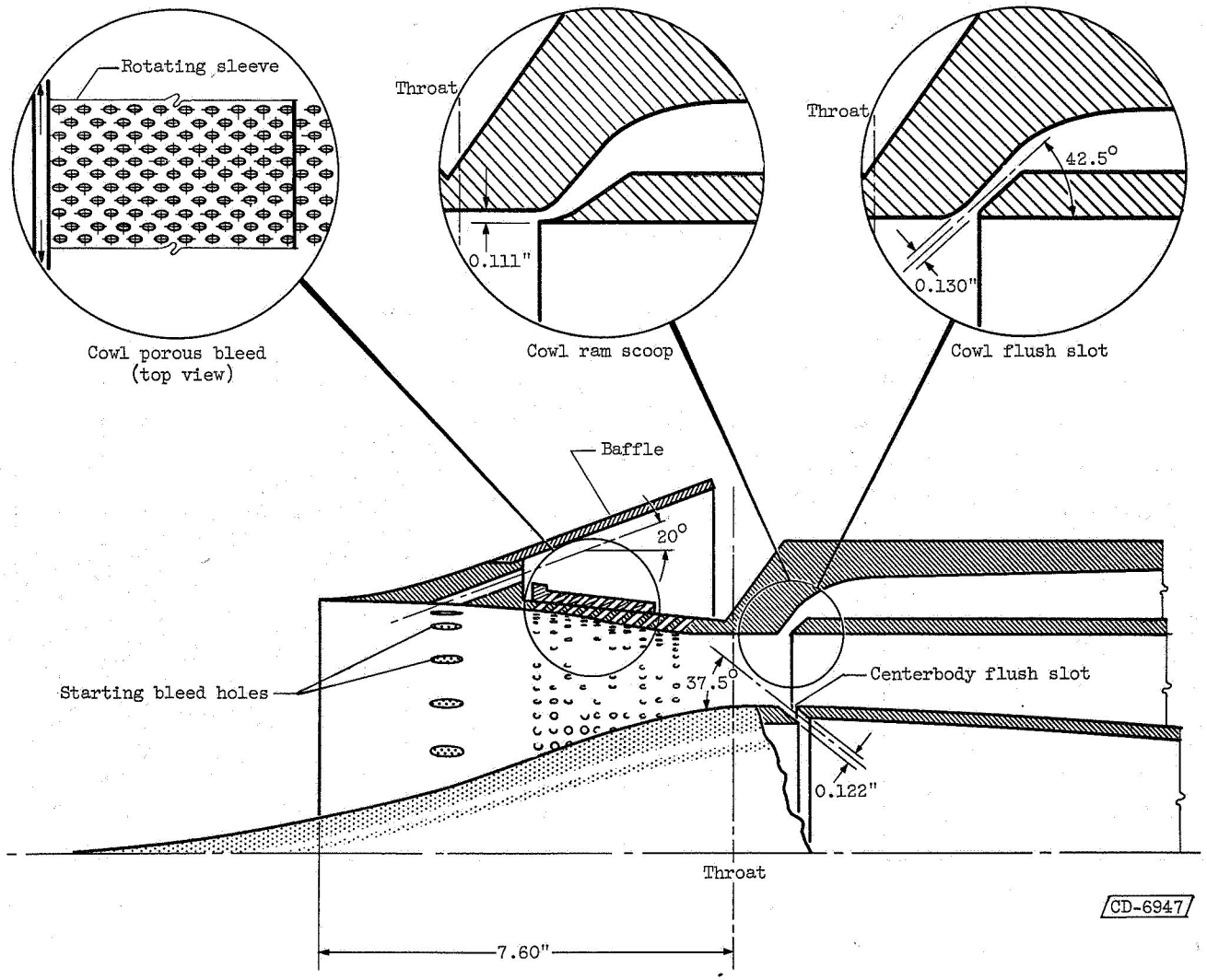

(c) Short supersonic inlet with bleed configurations (centerbody shown in design position).

Figure 2. - Concluded. Schematic diagrams of inlets investigated.

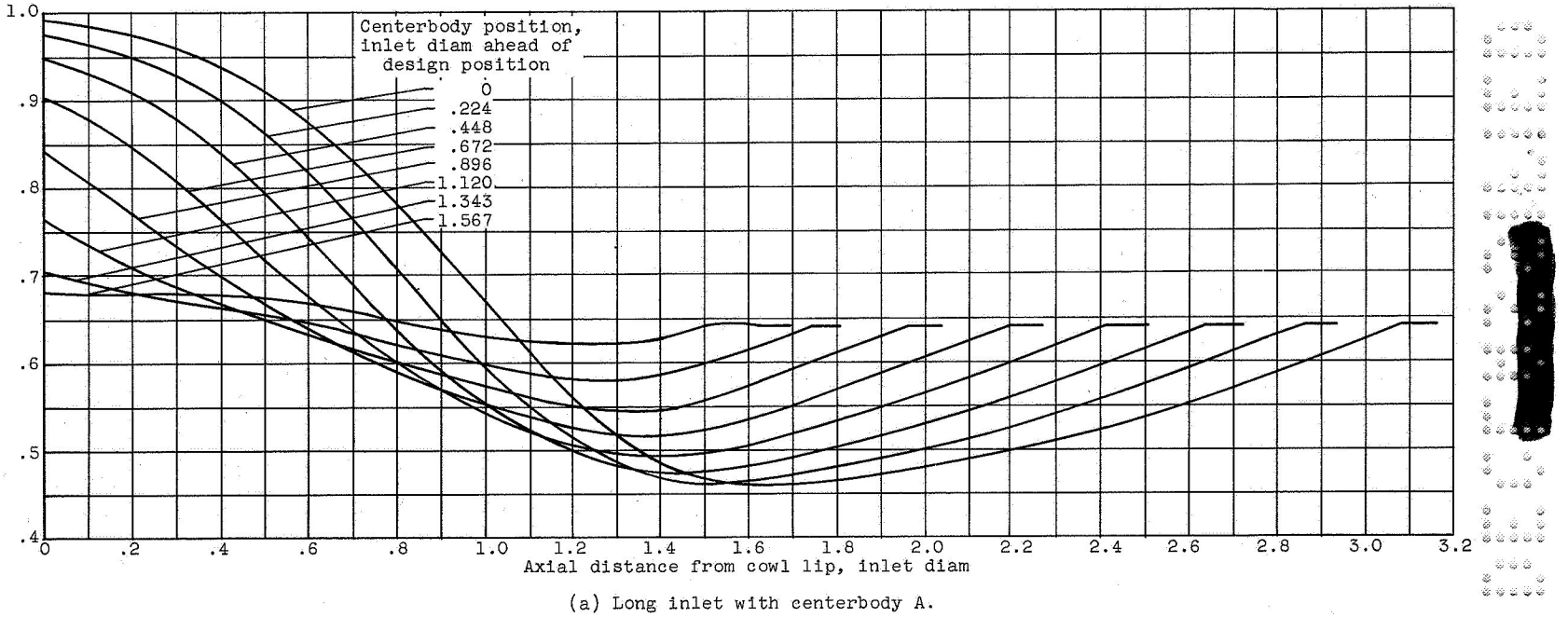

(a) Long inlet with centerbody A.

Figure 3. - Area distribution.

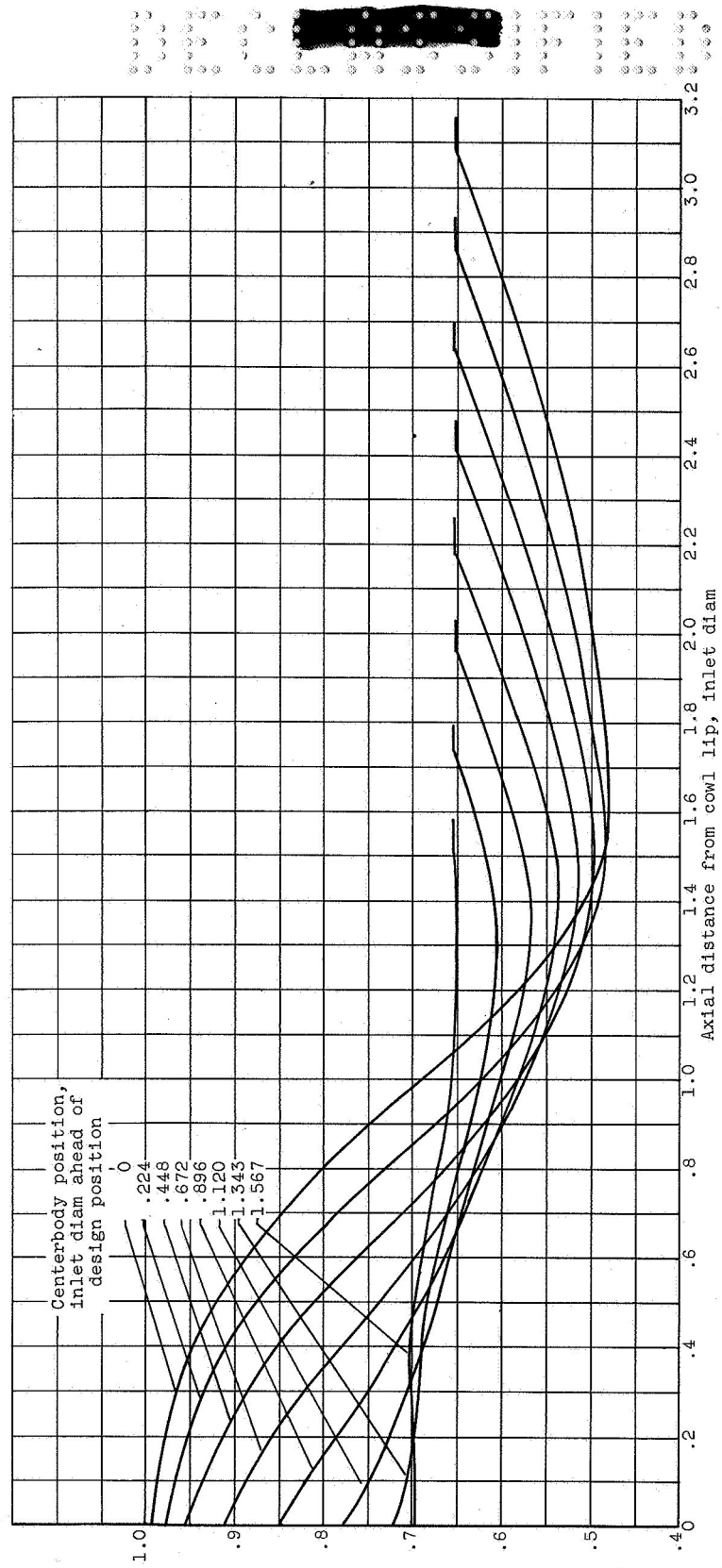

(b) Long inlet with centerbody B.

Figure 3. - Continued. Area distribution.

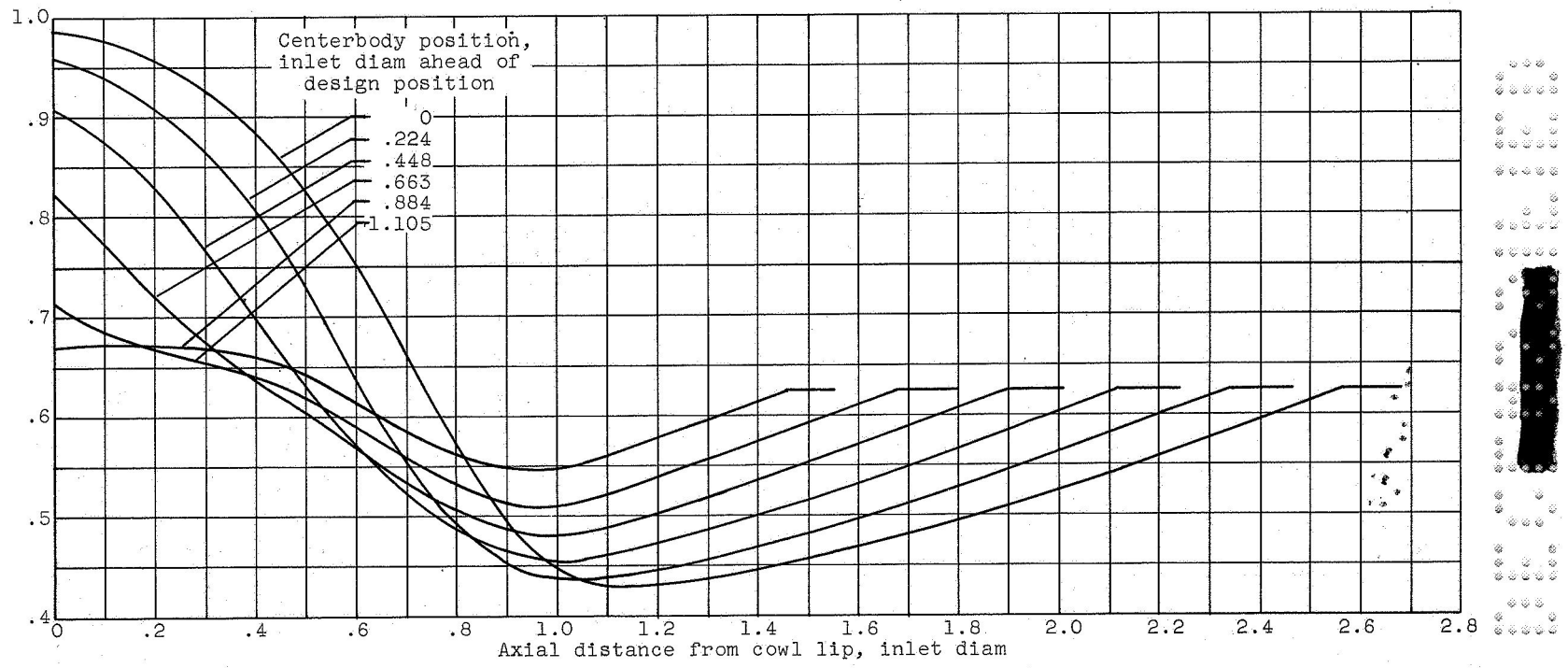

(c) Intermediate inlet.

Figure 3. - Continued. Area distribution.

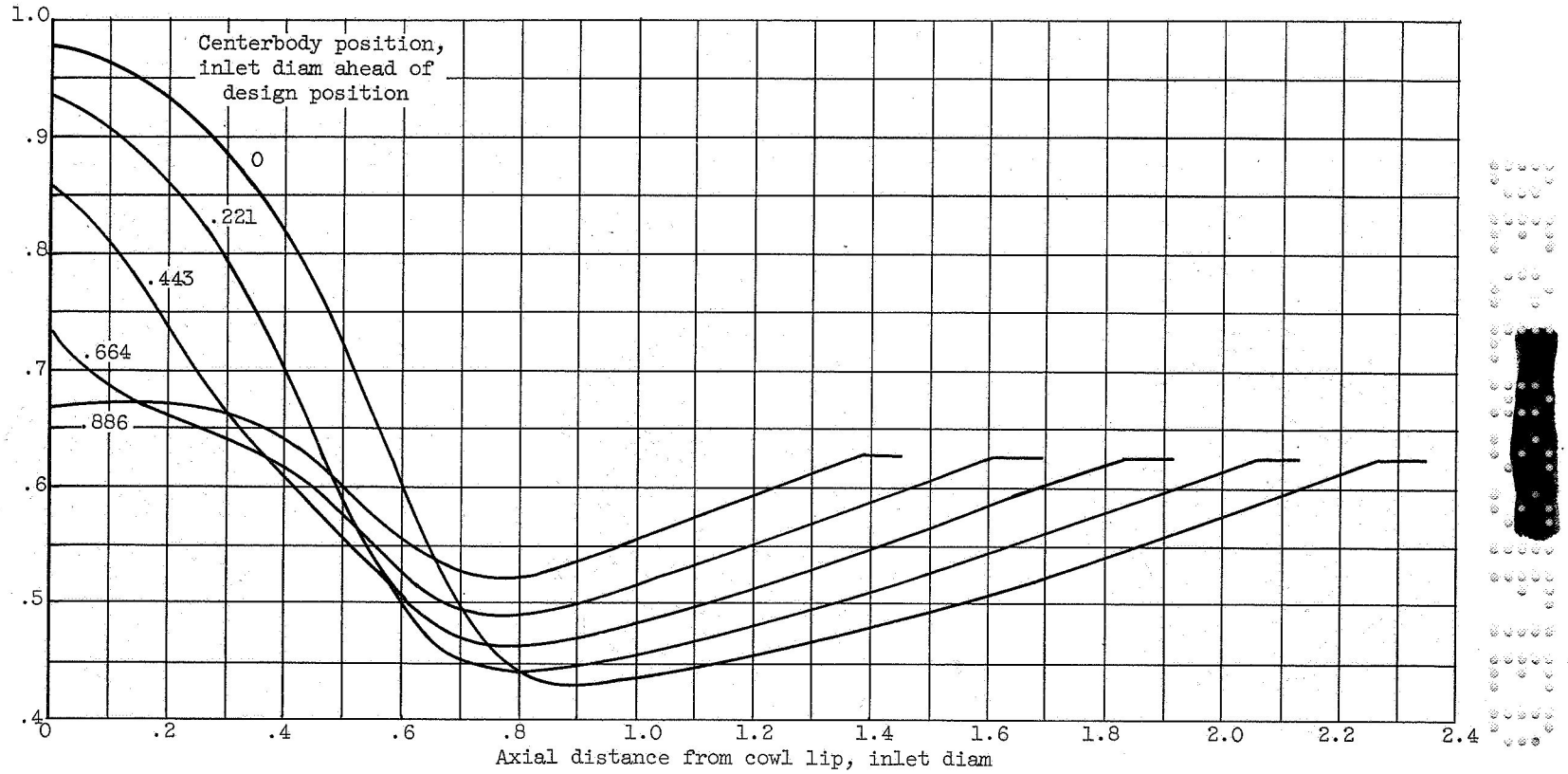

(d) Short inlet.

Figure 3. - Concluded. Area distribution.

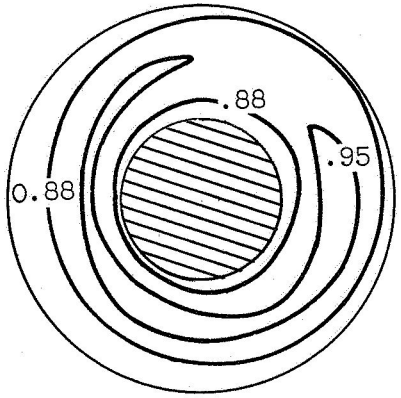

Long inlet
$P_2/P_0 = 0.904$
$\Delta P_2/\bar{P}_2 = 0.154$

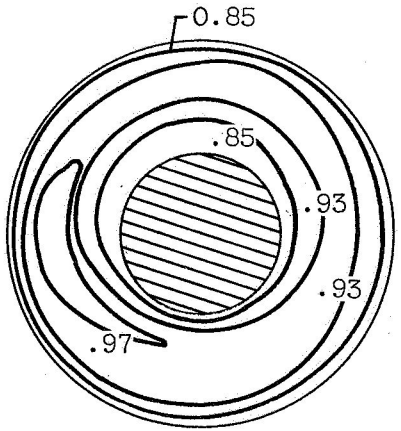

Intermediate inlet
$P_2/P_0 = 0.926$
$\Delta P_2/\bar{P}_2 = 0.148$

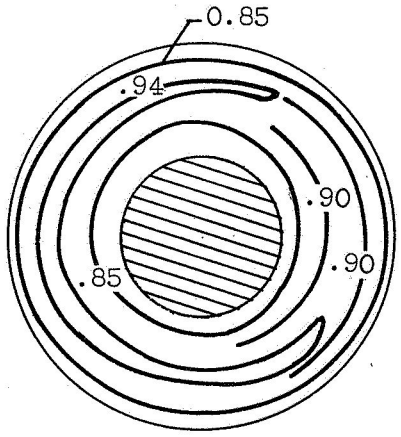

Short inlet
$P_2/P_0 = 0.886$
$\Delta P_2/\bar{P}_2 = 0.156$

Figure 4. - Diffuser-exit total-pressure contours at peak recovery for inlets with cowl ram bleed. Free-stream Mach number, 2.5; angle of attack, 0^o.

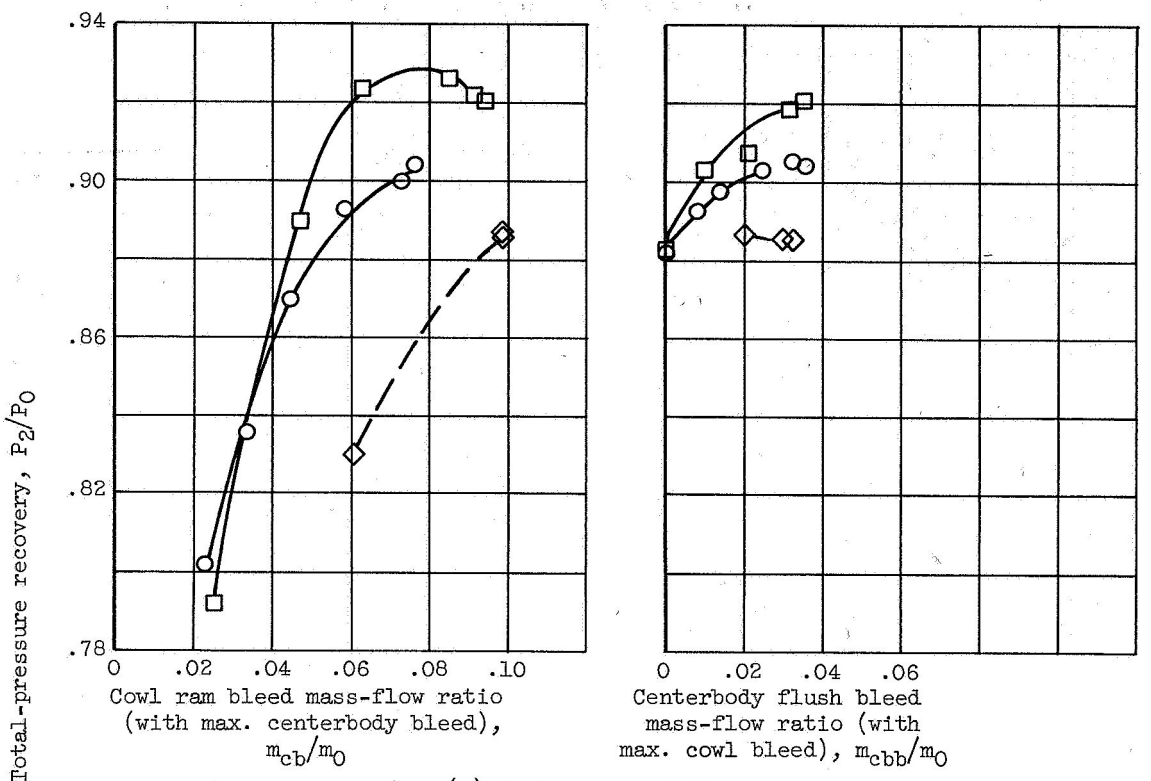

(a) Performance at Mach 2.5.

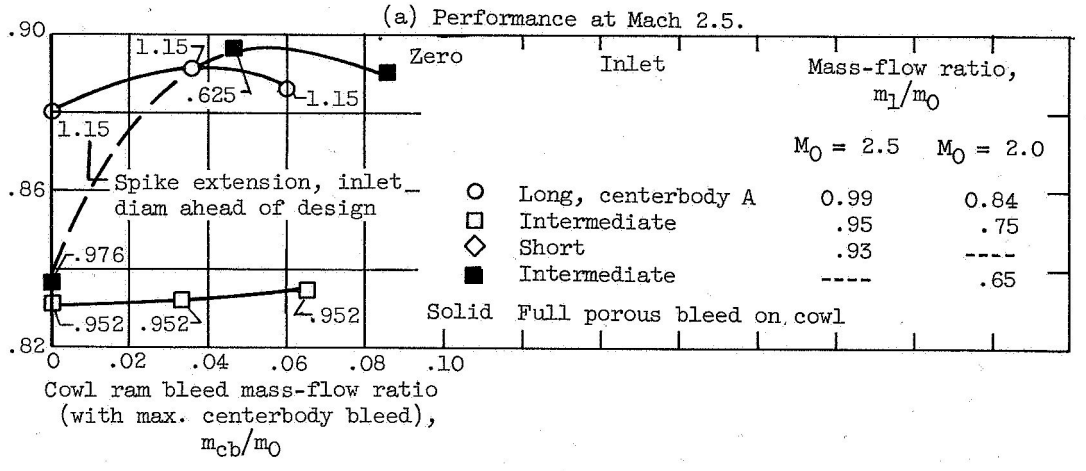

(b) Performance at Mach 2.0.

Figure 5. - Inlet performance with cowl ram bleed and centerbody flush bleed at 0° angle of attack.

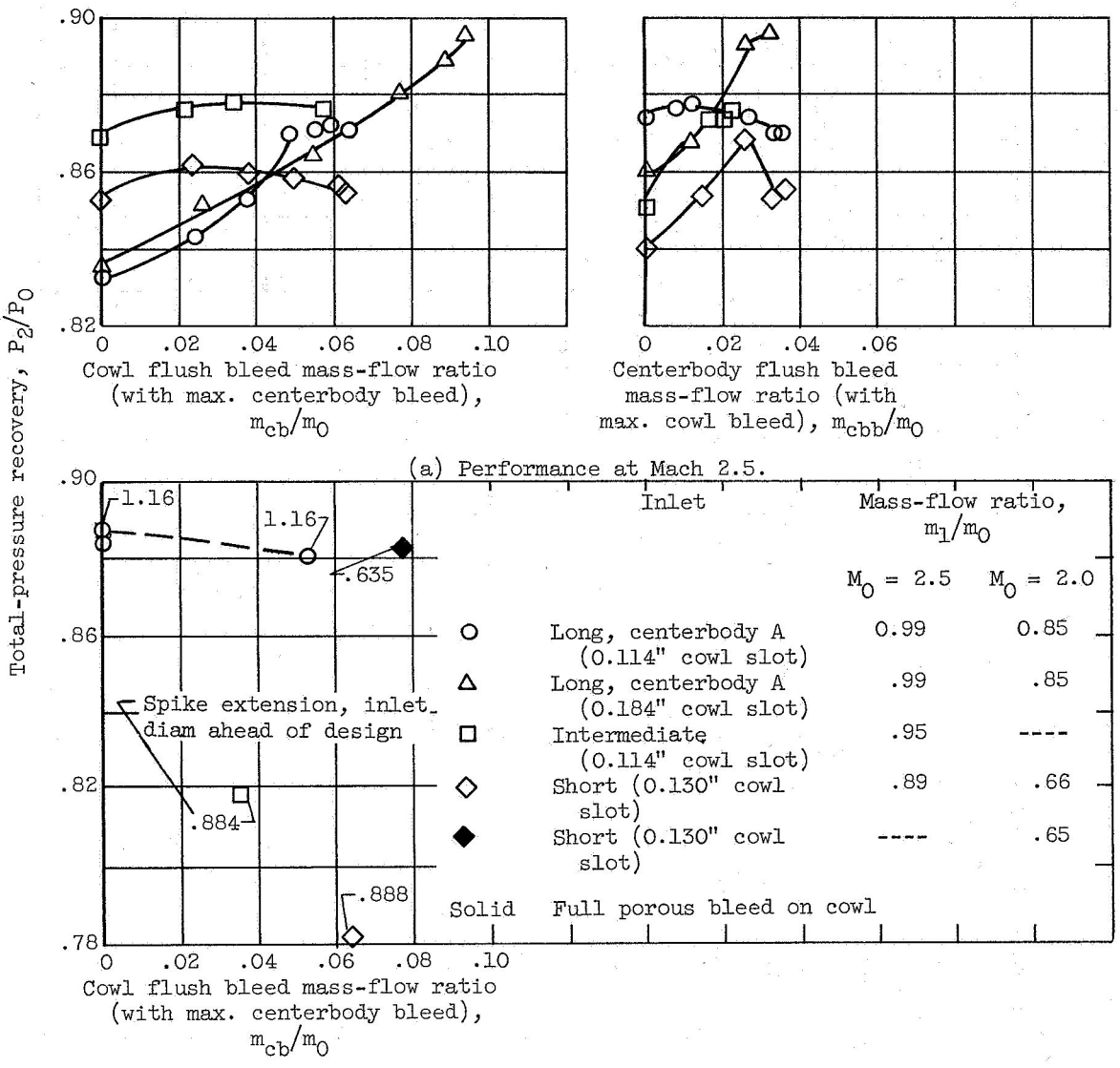

Figure 6. - Inlet performance with cowl and centerbody flush bleed at 0° angle of attack.

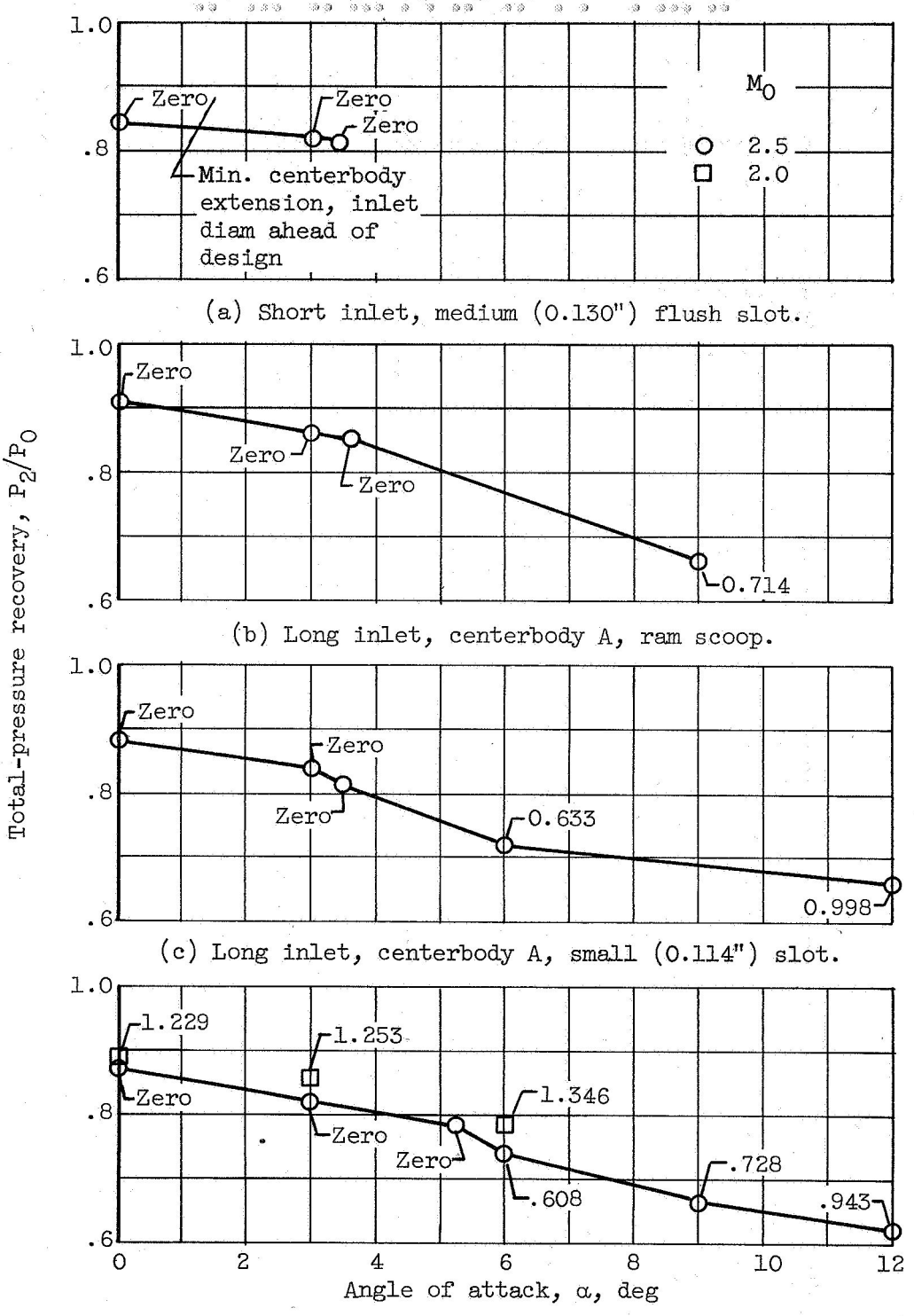

(a) Short inlet, medium (0.130") flush slot.

(b) Long inlet, centerbody A, ram scoop.

(c) Long inlet, centerbody A, small (0.114") slot.

(d) Long inlet, centerbody B, large (0.184") slot.

Figure 7. - Effect of angle of attack on maximum inlet pressure recovery.

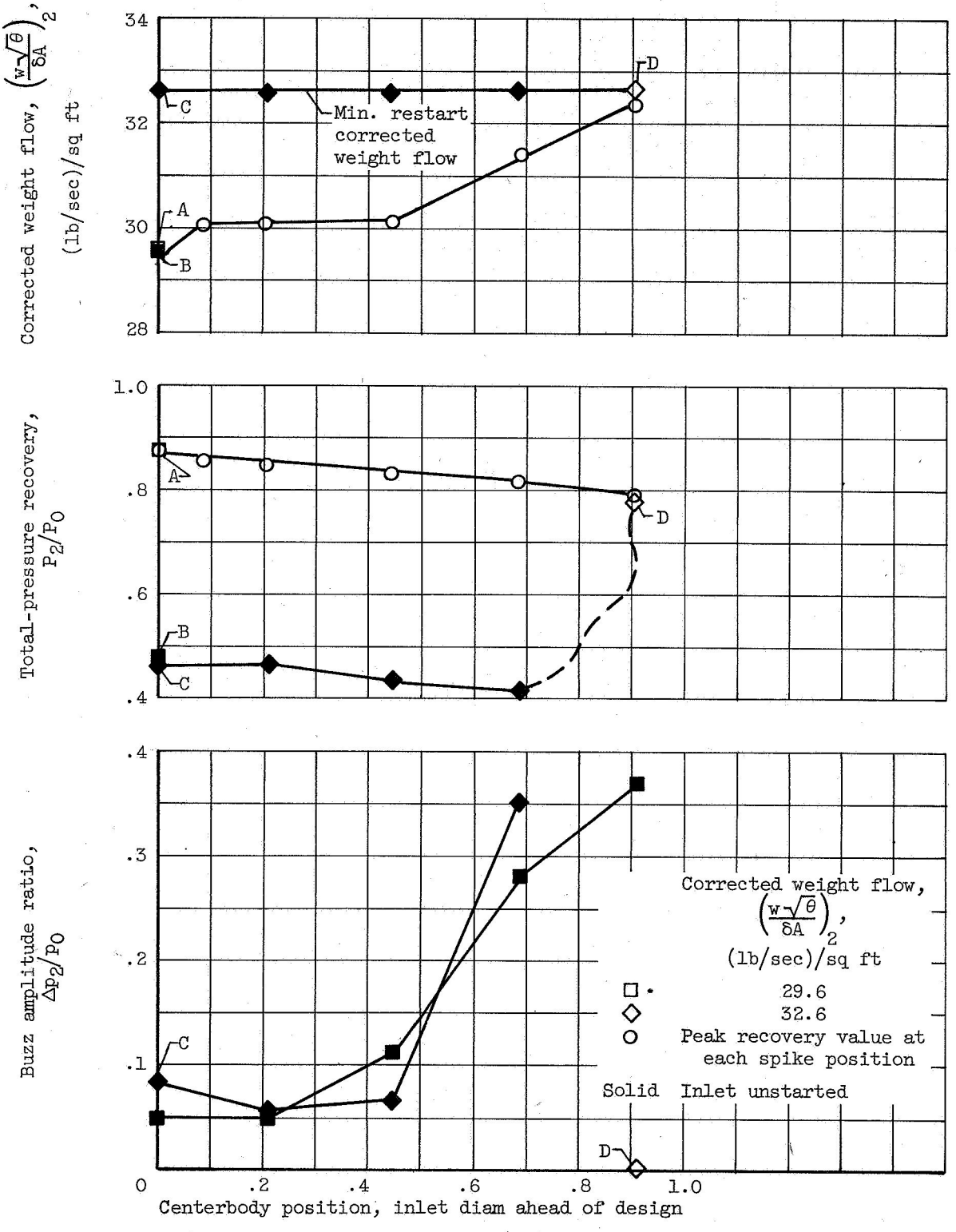

Figure 8. - Starting cycle for long inlet with centerbody B at Mach 2.5 and 0° angle of attack.

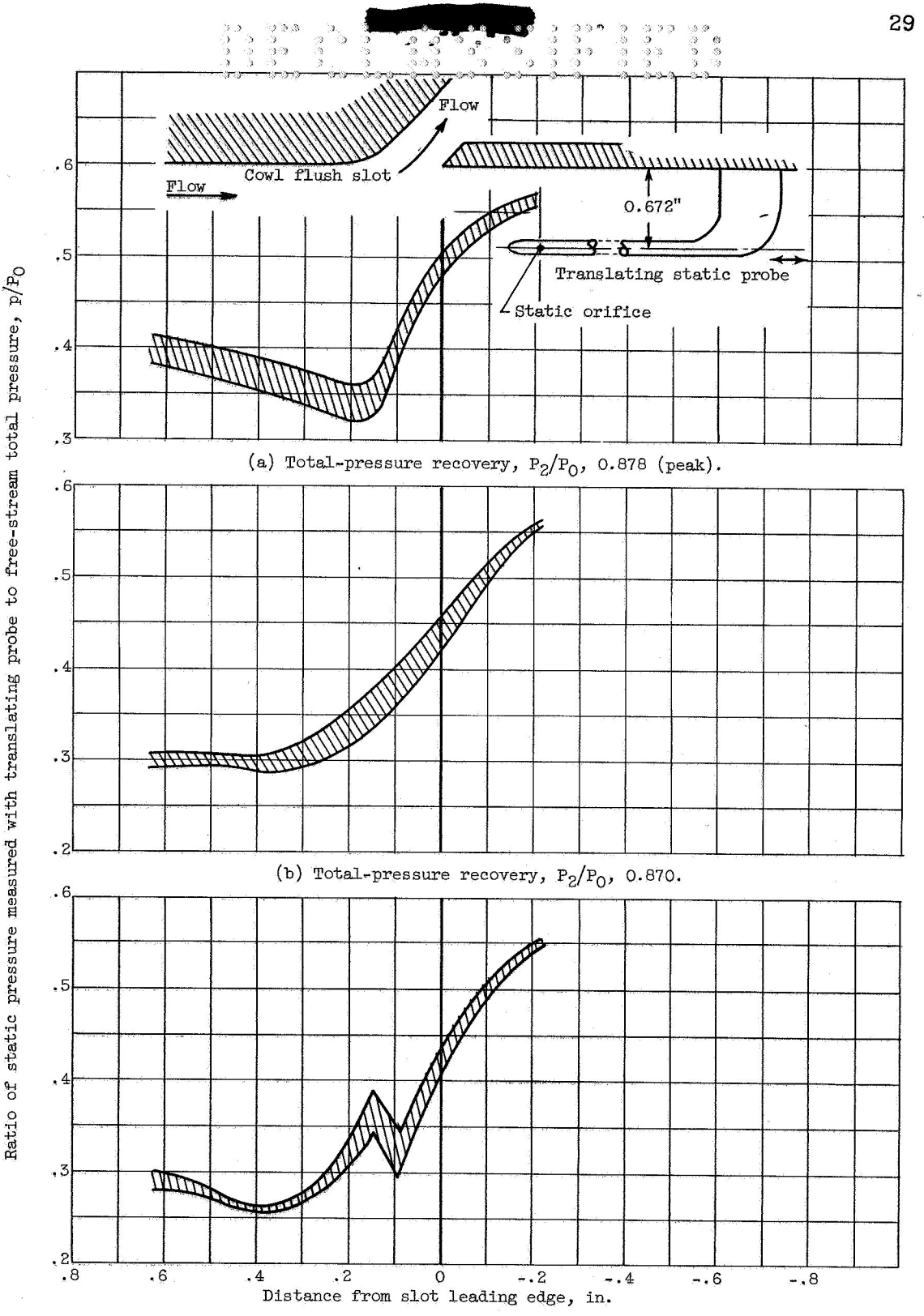

(a) Total-pressure recovery, P_2/P_0, 0.878 (peak).

(b) Total-pressure recovery, P_2/P_0, 0.870.

(c) Total-pressure recovery, P_2/P_0, 0.805.

Figure 9. - Stream static pressure in region of cowl slot. Long inlet at Mach 2.5.